Magnetic behaviour of $CuIn_{1-z}Fe_zS_2$

1992 J. Phys.: Condens. Matter 4 8221

(http://iopscience.iop.org/0953-8984/4/42/011)

J. Phys.: Condens. Matter 4 (1992) 8221–8232. Printed in the UK

Magnetic behaviour of $CuIn_{1-z}Fe_zS_2$

R Brun del Re, G Lamarche and J C Woolley

Ottawa-Carleton Institute for Physics, University of Ottawa, Ottawa, Ontario K1N 6N5, Canada

Received 2 April 1992, in final form 1 July 1992

Abstract. Single-phase polycrystalline samples of $CuIn_{1-z}Fe_zS_2$ ($0.04 < z < 0.6$) alloys with a chalcopyrite structure were studied by measurement of the low-field magnetic susceptibility χ and ESR in the temperature range 4–300 K, and by room-temperature Mössbauer spectroscopy. At the higher temperatures, the $1/\chi$ versus T data could be interpreted in terms of a modified Curie–Weiss relation, and values of the Curie–Weiss temperature Θ and Curie constant C were obtained. At lower temperatures, the $1/\chi$ versus T curves for each sample with $z > 0.2$ showed a minimum corresponding to a magnetic transition temperature T_c and the overall behaviour of the alloy system seems similar to the spin-glass form displayed by various semimagnetic semiconductor alloys containing Mn. The χ data show that, in the present system, the average magnetic moment of the Fe changes rather abruptly from a value corresponding to $S = \frac{5}{2}$ for $z < 0.05$ to $S = \frac{3}{2}$ for $z > 0.2$. However, the Mössbauer spectra indicate that the Fe remains in the Fe^{3+} state throughout the full composition range studied. The change in the magnetic moment is attributed to a change in the spin configuration of Fe^{3+}, and possible explanations for this are discussed.

1. Introduction

Crystalline semiconductors which contain transition elements as part of their lattice structure have received considerable attention in recent years. In many cases, the composition range of transition elements which can be included in a conventional semiconductor is quite wide and the materials can be looked upon as solid solutions or alloys between the conventional semiconducting compound and a magnetic compound (e.g. $Cd_{1-z}Mn_zTe$), and these materials have been labelled dilute magnetic semiconductors (DMSs). In other cases, the available range of solid solutions of transition elements resulting in a compound can be very narrow, although it is to be noted that some materials, such as I_2.Mn.IV.VI_4, have been labelled compounds when the composition range of the single-phase form is quite wide. This is frequently the case when VI ≡ Te. All these materials show interesting magnetic behaviour in addition to semiconducting behaviour, and it is convenient to label them semimagnetic semiconductors (SMSCs). One aspect of SMSC materials of current interest is concerned with the crystallographic ordering of the magnetic atoms and the resulting magnetic properties, such as large magneto-optical effects. Thus, in the case of the I_2.Mn.IV.VI_4 compounds, it has been suggested [1] that the magneto-optical effects could be very large as a result of the weaker antiferromagnetic interaction between the Mn atoms because the ordered structure allows no cation nearest-neighbour Mn

0953-8984/92/428221+12$04.50

atoms. Another aspect of this behaviour would be that high-T polarons could be sustained in some of these materials.

For SMSC alloys, those containing Mn as the magnetic component have received most attention to date [2]. However, some studies on SMSC alloys containing Fe, such as $Cd_{1-z}Fe_zTe$ [3], $Hg_{1-z}Fe_zTe$ [4] and $Cu.III_{1-z}Fe_zS_2$ [5, 6] alloys, have been published. The two different ionization states available to Fe can be expected to result in differences in the behaviour of the corresponding SMSC alloys. For Fe^{2+}, in the tetrahedral crystal field of the semiconductor lattice the ground state is $^6A_1$ (singlet), while the corresponding state for Fe^{3+} is $^1A_1$ (sextet), very similar to that of Mn^{2+}. Thus, it is of interest to compare the results of a study of Fe^{3+} SMSC alloys with those already obtained for Mn SMSC alloys (e.g. [7]).

Of the Fe^{3+} SMSC alloys, one obvious set for such a study is the chalcopyrite-type $I.III_{1-z}Fe_zVI_2$ alloys. Initial studies on polycrystalline samples of $CuIn_{1-z}Fe_zS_2$ [8], $CuGa_{1-z}Fe_zS_2$ [5] and $CuAl_{1-z}Fe_zS_2$ [6] have been reported, as have various magnetic and optical studies of the end member compound $CuFeS_2$ [9, 10]. In the present work, the low-field magnetic susceptibility, ESR and Mössbauer behaviour of polycrystalline samples of $CuIn_{1-z}Fe_zS_2$ alloys have been investigated. The crystallographic and phase diagram data for this system have been reported previously [8]. It was shown that the chalcopyrite phase exhibits room-temperature single-phase solubility ranges of $0 < z < 0.2$ and about $0.95 < z < 1.0$. However, it was found that, by quenching from a high-temperature zincblende phase field, room-temperature metastable samples with a chalcopyrite structure could be obtained over an appreciable range between the z limits given above of 0.2 and 0.95, thus appreciably extending the composition range over which the chalcopyrite behaviour could be investigated.

2. Sample preparation and experimental measurements

Polycrystalline samples were produced from the elements by the normal melt-and-anneal technique. The components of 1 g samples were sealed under vacuum in small quartz ampoules, heated to 1200 °C, kept at that temperature for approximately 30 min and cooled to room temperature. Next the resulting ingot was annealed at a chosen temperature for a minimum of 2 weeks and was then cooled to room temperature, either by rapidly quenching in brine or by gradually lowering the temperature in small steps over a period of approximately 2 weeks. The detailed treatment for each sample was determined from reference to the $T(z)$ phase diagram [8] and will be discussed further below. Each sample was then powdered and a Debye–Scherrer x-ray powder photograph taken to determine the condition of the sample.

For each single-phase sample, low-field static magnetic susceptibility measurements were made over the temperature range 4–220 K, using a SQUID apparatus described in detail previously [11], with a measuring static magnetic field of approximately 100 G. ESR studies were carried out on Bruker ER200D-SRC equipment with an associated ER043 MRD microwave bridge and a rectangular X-band cavity. Measurements were made both at room temperature and at lower temperatures, the latter being made with the use of an Air Products temperature regulator which stabilized the cavity temperature to within ± 2 K.

Room-temperature transmission Mössbauer spectra were taken with a 5 mCi ^{57}Co source in a rhodium matrix. The transducer was operated in constant-acceleration

mode and data were accumulated in 1024 channels. Calibration spectra were obtained with a ^{57}Fe-enriched iron foil before and after each spectrum and all line positions were given with respect to the centre of the calibration spectrum. The experimental spectra were folded to obtain a flat background. The important Mössbauer parameters can, to a good approximation, be obtained from the raw data but, to ensure consistency in the results, the data were analysed by least-squares fitting to simple Lorentzian line profiles.

3. Results and analysis

Zero-field-cooled susceptibility measurements were made on all the samples which showed the single-phase chalcopyrite condition. These included samples in the concentration range $0 < z < 0.2$ which had been very slowly cooled to room temperature and then annealed at 200 °C to give the equilibrium single-phase chalcopyrite condition and also samples in the range $0.2 < z < 0.6$ which had been rapidly quenched from 850 °C to give material showing the metastable chalcopyrite structure discussed previously [8]. The susceptibility apparatus used a self-compensating sample chamber which gave for the sample studied an estimated residual diamagnetic effect of the order of 10^{-8} emu g^{-1}. Since this was only 1% of the weakest measured susceptibility, diamagnetic corrections were neglected. The curves of $1/\chi$ versus T obtained for the various samples were of the form usually shown by antiferromagnetic and spin-glass materials. At the higher temperatures, $1/\chi$ showed an effectively linear variation with T, while for the higher z-values ($z > 0.2$) a peak in the value of χ, and hence a local minimum in $1/\chi$, was observed in the lower-temperature range. Since the samples with higher z were those quenched to a metastable form, the presence of strains and other effects of rapid quenching caused the minimum in $1/\chi$ to be blurred, and the usual sharp cusps associated with magnetic ordering temperatures were not observed. This is illustrated in figure 1, where curves of $1/\chi$ versus T in the range $4\,\mathrm{K} < T < 100\,\mathrm{K}$ are shown for four of the quenched samples. For the case of the first three samples in figure 1, the values of $1/\chi$ were obtained from measurements on zero-field-cooled samples. However, for the $z = 0.5$ sample (figure 1(*d*)), both zero-field-cooled and field-cooled data are given, clearly showing the temperature hysteresis for $T < T_c$. For the well annealed samples with $z < 0.2$, the minimum in $1/\chi$ would be below 4 K and so could not be observed. As discussed further below, this behaviour seemed to be typical of a spin-glass semiconductor, with a peak in χ representing the transition temperature T_c.

In the analysis of the behaviour of $1/\chi$ versus T, at sufficiently high values of T, a linear variation should be observed with the typical paramagnetic Curie–Weiss form, i.e. $1/\chi = (T-\Theta)/C$ and hence values of Θ and C could be determined. With the present results, such a linear form appears to be obtained in the higher-temperature range of observation. However, as indicated by Spalek *et al* [12], this linear form is strictly valid only for $T \gg |\Theta|$, which is not the case for the present data. Spalek *et al* showed that a first-order correction to the simple Curie–Weiss form can be obtained by considering the Θ/T-term in the expansion used in their analysis. From their results, the variation in $1/\chi$ with T can be written as

$$1/\chi = (1/C)(T - \Theta - P\Theta^2/T) \tag{1}$$

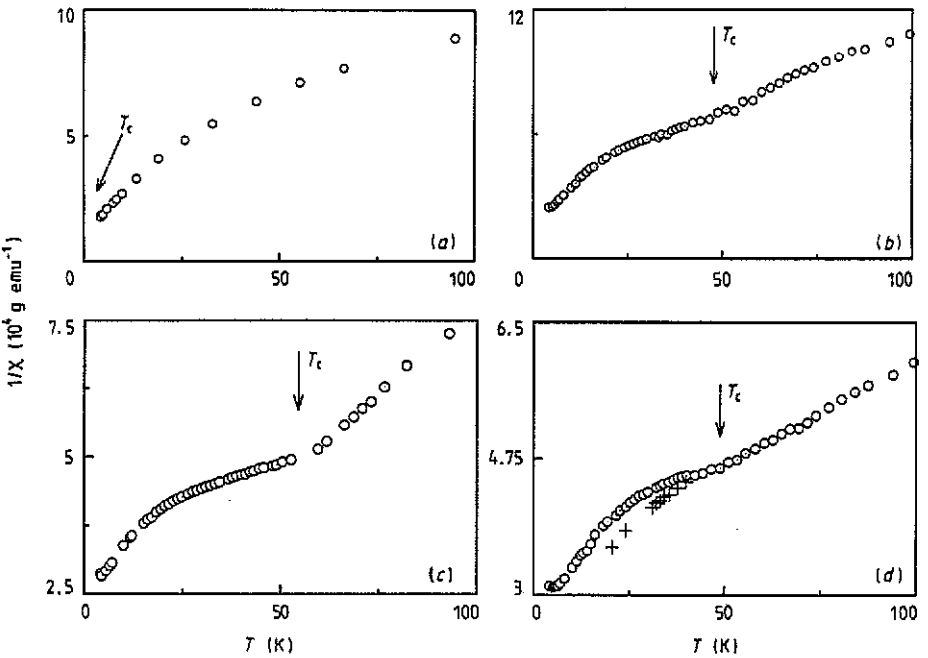

Figure 1. Temperature variation in the inverse susceptibility $1/\chi$ of various samples of $CuIn_{1-z}Fe_zS_2$ for temperatures in the range 4–100 K to show the occurrence of critical temperature T_c for (*a*) $z = 0.2$, annealed at 200 °C, (*b*) $z = 0.3$, quenched from 850 °C, (*c*) $z = 0.4$, quenched from 850 °C, and (*d*) $z = 0.5$, quenched from 850 °C: O, zero-field-cooled data; ×, field-cooled data.

where

$$P = 2\sum_i n_i J_i^2 \Big/ \left(\sum_i n_i J_i\right)^2 \tag{2}$$

J_i being the value of the exchange parameter for a pair of ith cation neighbours and n_i being the number of cations on the ith coordination sphere.

The variations in $1/\chi$ with T obtained in the present work for a number of typical samples are shown in figure 2. These were analysed in the temperature range well above T_c (as indicated in figure 2) in terms of equation (1) using a standard nth-order regression programme to give values for C, Θ and P. The values of T_c, Θ, C and P obtained for the various samples are listed in table 1 and the values of Θ, T_c and P are shown plotted against z in figures 3, 4 and 5, respectively. Because of the blurring of the $1/\chi$ minima indicated above, the T_c-values show some experimental scatter, while the limited temperature range over which the behaviour of $1/\chi$ versus T could be analysed resulted in a similar experimental scatter in the observed Θ, C- and P-values.

ESR measurements were made on a number of the single-phase samples in the temperature range from 10 to 300 K. A typical set of derivative spectra at various temperatures for a low-temperature-annealed sample with $z = 0.2$ are shown in figure 6. These spectra show a single resonance line at $g = 2.0$ with a peak-to-peak linewidth ΔH as indicated in the figure. The variation in ΔH with temperature in

Table 1. Magnetic parameters for $CuIn_{1-z}Fe_zS_2$. T_c is the magnetic transition temperature, Θ the Curie–Weiss temperature, C the Curie constant, P the Curie–Weiss correction parameter, $\sum$ the sum of exchange interactions per magnetic ion and S the spin value. The estimated random errors are generally less than 15% and are shown on the appropriate graphs.

z	T_c (K)	$-\Theta$ (K)	C (10^{-4} emu K g^{-1})	P	$\sum$ (K)	S
0.04	—	70	6.04	0.179	373	2.24
0.06	—	95	7.53	0.175	398	2.00
0.08	—	102	7.72	0.139	408	1.70
0.10	—	134	13.2	0.096	424	2.05
0.15	—	155	14.5	0.115	360	1.68
0.20	—	192	16.9	0.128	315	1.54
0.30	38	329	34.9	0.052	321	1.84
0.40	60	289	35.7	0.096	264	1.54
0.50	50	319	51.8	0.053	215	1.66
0.60	65	318	52.6	0.050	209	1.47

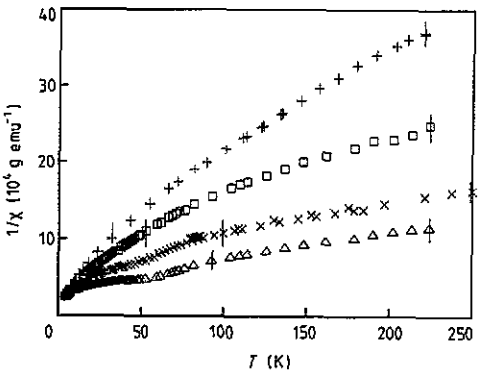

Figure 2. Temperature variation in the inverse susceptibility $1/\chi$ of various samples of $CuIn_{1-z}Fe_zS_2$: +, $z = 0.06$, annealed at 200 °C; □, $z = 0.10$, annealed at 200 °C; ×, $z = 0.3$, quenched from 850 °C; △, $z = 0.4$, quenched from 850 °C. The vertical lines indicate the ranges of temperature over which the analysis was carried out.

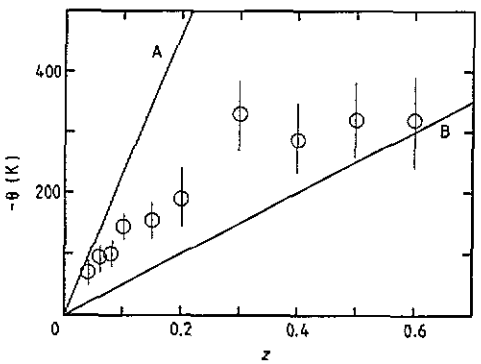

Figure 3. Variation in the Curie–Weiss temperature Θ with z for $CuIn_{1-z}Fe_zS_2$: line A, Θ-values for $S = \frac{5}{2}$, $\sum_i n_i J_i = 400$ K; line B, Θ-values for $S = \frac{5}{2}$, $\sum_i n_i J_i = 200$ K.

this case is shown in figure 7. For the case when $0.2 < z < 0.6$, the only single-phase chalcopyrite samples were the metastable samples produced by rapid quenching from 850 °C. As seen from the crystallographic work [8], the larger-angle x-ray lines for these samples were blurred, indicating some degree of inhomogeneity as would be expected from the method of production. For these samples, the ESR spectra showed a similar behaviour, the resonance line being very blurred. Thus values for the linewidth ΔH could not be obtained in these cases, but it was clear that for all the alloys the value of g was close to 2.0.

Typical Mössbauer spectra for single-phase chalcopyrite samples are given in figure 8. Curves are shown for the alloys with $z = 0.1$ and 0.15 which had been annealed

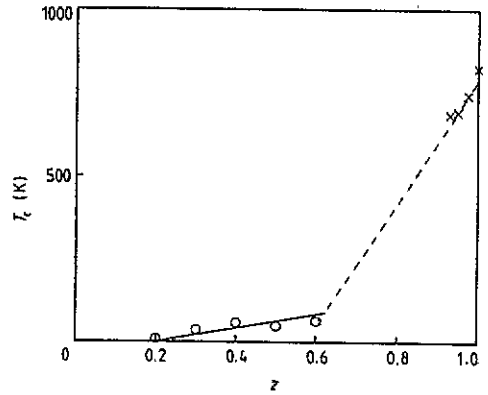

Figure 4. Variation in magnetic critical temperature T_c with z for $CuIn_{1-z}Fe_zS_2$ alloys: O, susceptibility data; X, DTA data [8].

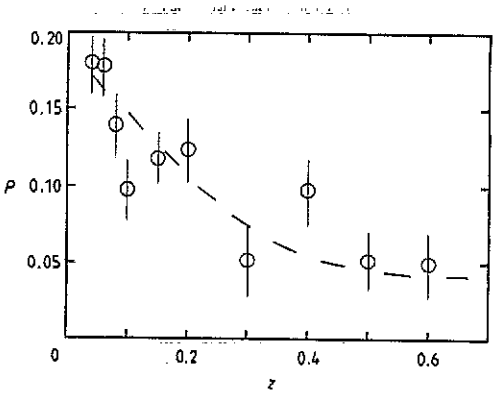

Figure 5. Variation in Curie–Weiss correction factor P with z for $CuIn_{1-z}Fe_zS_2$ alloys.

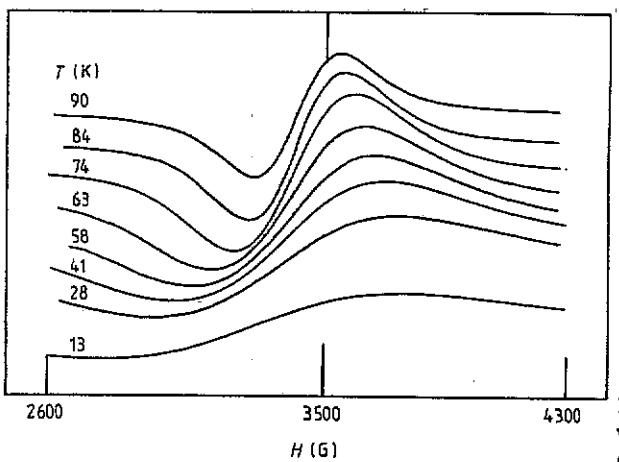

Figure 6. ESR spectra for $CuIn_{1-z}Fe_zS_2$ with $z = 0.2$ at the temperatures indicated.

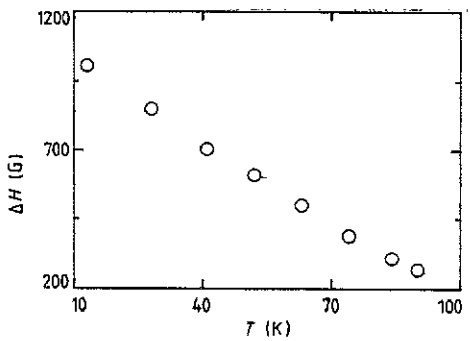

Figure 7. Variation in the ESR linewidth ΔH with temperature for $CuIn_{1-z}Fe_zS_2$ with $z = 0.2$.

at 200 °C (figures 8(*a*) and 8(*b*)) and for the alloys with $z = 0.1$ and 0.4 which had

been quenched from 850 °C (figures 8(*c*) and 8(*d*)). For comparison purposes, the spectrum of a $z = 0.4$ alloy annealed to two-phase equilibrium at 200 °C is also shown (figure 8(*e*)). Two Mössbauer parameters which are of interest in the present work can be determined from these curves, these being the quadrupole splitting parameter Δ and the centre shift parameter δ, both of which represent interaction energies. The dominant contribution to the first four spectra shown in figure 8 is a narrow quadrupole doublet (labelled A) with $\Delta = 0.2$ mm s^{-1} and $\delta = 0.3$ mm s^{-1}. This is the accepted response for Fe^{3+}. Within the limits of experimental error, the values of Δ and δ remained constant in the measured concentration range ($0 < z < 0.7$). One other contribution to the spectra of the single-phase alloys is the quadrupole doublet with $\Delta = 2.2$ mm s^{-1} and $\delta = 0.6$ mm s^{-1}, which has a much smaller intensity than the previous case and again is effectively constant in the range of measurement ($0 < z < 0.3$). This doublet, labelled B in figure 8, can be attributed to Fe^{2+} which appears to be present in quite small amounts in the low-temperature-annealed alloys but in larger amounts in the alloys quenched from 850 °C, as can be seen from a comparison of the spectra of the two cases with $z = 0.1$ shown. This will be discussed further below. In the low-temperature-annealed two-phase alloy, the spectra of the two phases can clearly be seen, namely the doublet A due to the In-rich phase and the sextet (labelled C) due to the Fe-rich chalcopyrite phase which is antiferromagnetic and below its Néel temperature at room temperature. Again, comparison of the two $z = 0.4$ cases given in figure 8 clearly shows the difference produced by the two different heat treatments in this case and confirms the observation from the x-ray data that the quenching from 850 °C produces a metastable single-phase chalcopyrite form. One other structure was observed in the Mössbauer spectra for the case of the high-z alloys close to $CuFeS_2$, where in addition to the expected sextet of $CuFeS_2$ the quadrupole doublet of FeS_2 was observed. This again is in agreement with the x-ray and phase diagram results [8], which showed that at temperatures in the vicinity of 600 °C these Fe-rich alloys decompose into a zincblende phase plus a small amount of FeS_2. It was found that, even when these alloys were quenched from higher temperatures and then annealed at lower temperatures for several weeks, traces of FeS_2 were still observed in the x-ray photographs.

4. Discussion

In the analysis and discussion of the data presented above, the first question which needs to be answered is the state of the Fe atoms, whether they are in the triply ionized (Fe^{3+}) or doubly ionized (Fe^{2+}) state. There has been some disagreement in the literature as to the case for $CuFeS_2$ [13, 14], but the present Mössbauer data indicate that, as far as the alloys in the range $0 < z < 0.6$ are concerned, the large majority of the Fe atoms are Fe^{3+}, the values of $\Delta = 0.2$ mm s^{-1} and $\delta = 0.3$ mm s^{-1} clearly indicating this. This conclusion is supported by the ESR data, where the presence of a single resonance line at $g = 2$ is consistent with the presence of Fe^{3+} [15]. Fe^{2+}, if present, would not be expected to produce a visible ESR line under the present conditions of measurements [15]. As indicated above, the Mössbauer spectra do show a small component characteristic of Fe^{2+}, with the amount varying with the method of production of the alloy and the value of z. The least-squares fitting of the Mössbauer spectra to simple Lorentzian lineshapes gives a good estimate of the relative amounts of Fe^{3+} and Fe^{2+} in each case. It was found that the Fe^{2+}-to-Fe^{3+}

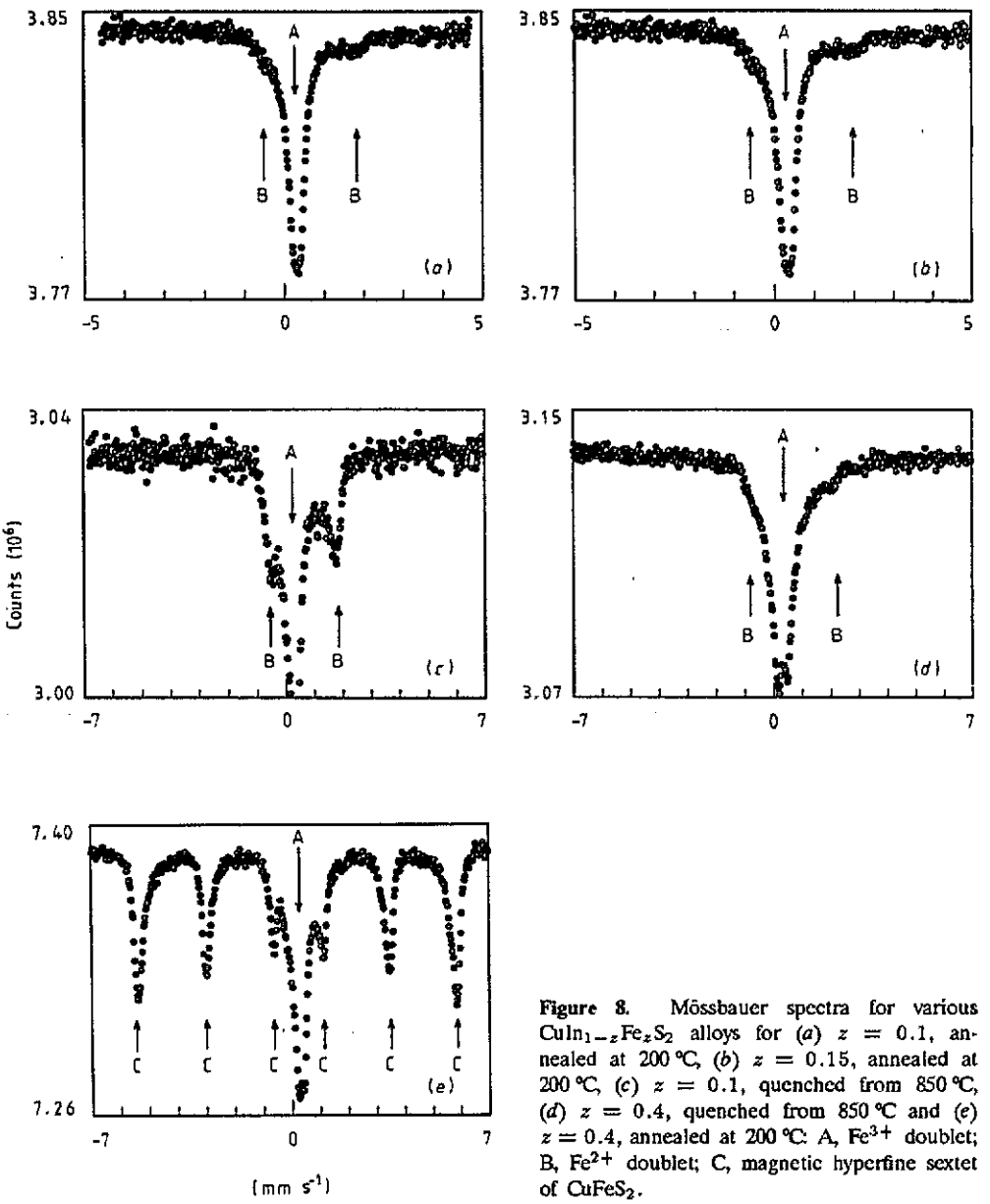

Figure 8. Mössbauer spectra for various $CuIn_{1-z}Fe_zS_2$ alloys for (*a*) $z = 0.1$, annealed at 200 °C, (*b*) $z = 0.15$, annealed at 200 °C, (*c*) $z = 0.1$, quenched from 850 °C, (*d*) $z = 0.4$, quenched from 850 °C and (*e*) $z = 0.4$, annealed at 200 °C: A, Fe^{3+} doublet; B, Fe^{2+} doublet; C, magnetic hyperfine sextet of $CuFeS_2$.

ratio did not in any sample exceed 10% and in the low-temperature-annealed alloys was considerably smaller than this.

The presence of larger amounts of Fe^{2+} in the quenched samples suggests that the occurrence of Fe^{2+} is related to site defects in the chalcopyrite lattice. At the quenching temperature (850 °C), the structure is zincblende with the Cu, In and Fe atoms arranged at random on the cation sublattice. With rapid quenching, there is not time for the alloy to separate into two phases (a long-range effect), but ordering of the cations (a short-range effect) can occur. However, this ordering is unlikely to

be complete and, as a result, some Fe ions will remain on Cu sublattice sites with a corresponding number of Cu ions on the In/Fe sites. When a sample is annealed at low temperatures, this number of site defects will be reduced but will not become zero. It is suggested that these Fe ions on Cu sites will take the Fe^{2+} form, and to conserve the available valence band electrons the Cu on In/Fe sites will become Cu^{2+}. An occurrence of Fe^{2+} in this manner would fit the present experimental data well. The values of the Fe^{2+}-to-Fe^{3+} ratio were found to decrease with increasing z and the values indicate that the Fe^{2+} concentration tends towards saturation as z is increased. The resulting reduction in the relative amplitude of the Fe^{2+} peaks with increased z can be seen in the spectra in figure 8. It was also found that for the quenched samples of higher z-value, as well as being reduced, the Fe^{2+} peak is blurred. One suggested explanation of this is charge transfer between adjacent Fe^{2+} and Fe^{3+} ions on the cation sublattice, since such charge transfer could blur the spectra of both of the ions involved. Because of the relatively small concentrations, this would have little effect on the Fe^{3+} spectra observed but would have a large effect in the Fe^{2+} case.

Turning to the magnetic data, as indicated above, values were determined for the Néel temperature T_c, the Curie–Weiss temperature Θ and the Curie constant C using the modified form of the Curie–Weiss equation given in equation (1). As indicated above, this equation was used because the linear Curie–Weiss equation is strictly valid only for $T \gg |\Theta|$. The question of the temperature range over which the modified equation applies cannot be given explicitly since, as is seen from equation (1), this depends upon the value of P which is a property of the particular material being investigated. In the present analysis, as is seen from table 1, the magnitude of P was of the order of 0.1. Values were calculated for the correction term $P\Theta^2/T$ for all cases analysed and it was found that the resulting correction was never more than 15% and was in most cases appreciably smaller than this. With correction terms of this size, it would appear that the use of equation (1) is reasonable for the present data. It is to be noted that, in the analysis by Spalek *et al* [12] of $1/\chi$ data for alloys such as $Cd_{1-z}Mn_zTe$ and $Cd_{1-z}Mn_zSe$, satisfactory values of Θ and C were obtained from analysis of data in the range $T < |\Theta|$, and that similar results were obtained by the present authors [16] in a similar analysis of the corresponding ternary alloys. It is suggested that for the Mn alloys the values of P are appreciably smaller than the values obtained here, so that the correction terms in the Curie–Weiss equation are correspondingly smaller and so the linear form of the Curie–Weiss equation can effectively be used in a lower-temperature range than the strict theoretical limit of $T \gg |\Theta|$.

In the present work, the value of C is related to p_{eff}, the effective average magnetic moment, and hence to J, the average total spin of the Fe ions [17], i.e.

$$C = p_{\text{eff}}^2\beta^2/3k_B \text{ per magnetic ion} \tag{3}$$

where

$$p_{\text{eff}} = g[J(J+1)]^{1/2}. \tag{4}$$

The ESR data show that, for all the samples concerned here, $g = 2.0$, which indicates that the orbital contribution is quenched, i.e. $L = 0$, as may be expected for materials of this type [18], and thus $J = S$, the total spin contribution. Hence equations (3) and (4) can be rewritten as

$$C = zN_Ag^2\beta^2S(S+1)/3k_BW \text{ emu K g}^{-1} \tag{5}$$

where N_A is Avogadro's number and W is the molecular weight. Thus the values of S were determined from the experimental C-values, and these are shown as a function of z in figure 9.

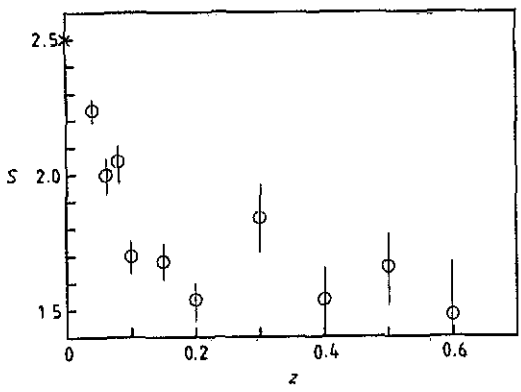

Figure 9. Variation in S with z for $CuIn_{1-z}Fe_zS_2$ as determined from susceptibility data: x, value for the compound [24].

For the concentration range $0 < z \lesssim 0.05$, S has the value of $\frac{5}{2}$, which is the value to be expected for Fe^{3+}. However, with further increase in z, S falls rapidly and for $0.2 < z < 0.7$ the present results show S to have a value approaching $\frac{3}{2}$ which is in good agreement with the value quoted for $CuFeS_2$ [17]. This latter value was determined from neutron diffraction work and not from measurements of magnetic susceptibility, so that the problems of the correct form for the variation in $1/\chi$ with T did not apply in that case. The variation in the values of S with z previously reported for the $CuGa_{1-z}Fe_zS_2$ [5] and $CuAl_{1-z}Fe-zS_2$ [6] alloys show a similar form to that reported above, but in those cases the S-values are reported only in the approximate range $0 < z < 0.2$, so that the fall in S to a value close to $\frac{3}{2}$ is not clearly seen. In the present work, this lower average value of S cannot be attributed to the presence of Fe^{2+} ions since, as indicated above, the fraction of Fe in the Fe^{2+} state is always less than 10% and thus the lower value of S must be due to Fe^{3+} ions.

For isolated Fe^{3+} ions, there are various possible spin configurations. When tetrahedrally coordinated and in a weak crystal field, the lowest state is $^6A_1$ which gives $S = \frac{5}{2}$, but other higher-energy spin configurations are possible, e.g. $^4T_1$ which gives $S = \frac{3}{2}$. It has been shown [18] that, as the crystal field increases, the relative energy values change and crossover can occur so that an increased effective crystal field could explain the present data. However, that analysis was for pure d-state conditions and another factor, namely p–d hybridization, must be considered in the present case. Significant mixing of noble metal d character occurs in the valence band of non-magnetic chalcopyrite materials such as $I.III.VI_2$ [20] and p–d mixing has also been shown to be important in Mn SMSCs such as $Cd_{1-z}Mn_zSe$ [21]. Any p–d mixing is considered to lower the energy of the participating magnetic orbitals and thus result in a greater tendency for spin pairing of the d electrons. Similarly, π bonding between the metal d and sulphur p orbitals, which has been considered to result in the low-spin states found in octahedrally coordinated sulphides, can also occur to some extent in tetrahedral sulphide complexes [22]. Such effects could be responsible for the increased tendency towards spin pairing seen here.

For the $CuIII_{1-z}Fe_zS_2$ alloys, in the vicinity of $z = 0.1$, delocalization of the Fe^{3+} d states occurs [6] to give a narrow d band, and this allows significant hybridization of the Fe^{3+} d states with the p states of the valence band, so that the valence band acquires some d character and the Fe^{3+} states take on some p character. In terms of a bonding picture, this means that the sp^3 hybridized bonding orbitals acquire some admixture of sd^3 behaviour. The addition of p character to the Fe^{3+} states will tend to favour paired spins and also will result in the bonding orbitals in a displacement of the average charge towards the Fe^{3+} ions, which will cause the crystal field at those ions to be increased. These various effects, which will increase as z increases, will all favour spin pairing and could thus have the result that the average value of S is $\frac{3}{2}$ for $z > 0.2$. In the intermediate transition range, about $0.05 < z < 0.2$, the effects would be more complicated, with the spin configurations of the Fe^{3+} ions possibly being a function of temperature as well as z. The scatter of points in this range, as seen in figure 9, is thus not unexpected.

The form of the Θ versus z curve shown in figure 3 also reflects the change in S with increased z. From standard mean-field theory [23], the value of Θ is given by

$$\Theta = \frac{2S(S+1)}{3k_B} z \sum_i n_i J_i. \tag{6}$$

For fixed values of S and $\sum_i n_i J_i$ the variation in Θ with z should be linear. Values of $\sum_i n_i J_i$ can be determined in the present case from the experimental data. From equations (3) and (4),

$$\sum_i n_i J_i = \frac{\Theta}{C} \frac{N_A g^2 \beta^2}{2W}. \tag{7}$$

From the experimental values of Θ and C given in table 1, values of $\sum_i n_i J_i$ were obtained and these are shown as a function of z in figure 10.

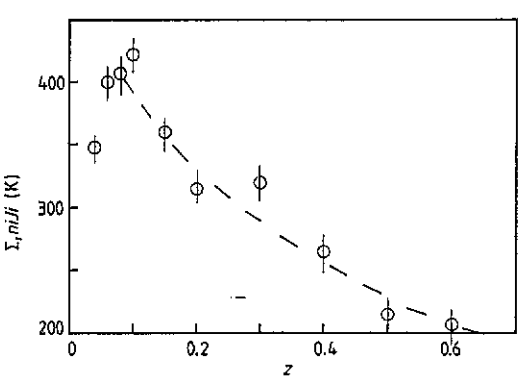

Figure 10. Variation in $\sum_i n_i J_i$ with z for $CuIn_{1-z}Fe_zS_2$ determined from susceptibility data.

It is seen that the values of $\sum_i n_i J_i$ show a fairly smooth fall from approximately 400 K at $z = 0$ to approximately 200 K at $z = 0.6$. The values of n_i remain the same throughout this range, but the values of J_i can change appreciably, since there is a change in ionic spacing as seen from the variation in the lattice parameter with z, and also since the details of the exchange mechanism may change when delocalization of

the d states occurs. It is seen from figure 4 that the values of P, which also depend upon the value of J_i, show a variation with z very similar to that shown by $\sum_i n_i J_i$. When values of $S = \frac{5}{2}$ and $\sum_i n_i J_i = 400$ K, corresponding to the conditions at $z = 0$, and $S = \frac{3}{2}$ and $\sum_i n_i J_i = 200$ K, corresponding to $z = 0.6$, are substituted into equation (6), two limiting straight lines are obtained as shown in figure 3, and the values of Θ are seen to move from one to the other as z increases.

Figure 4 shows the measured variation in T_c with z. As indicated above, there is appreciable scatter in the values but to a reasonable approximation the variation can be represented by a straight line which falls below 4 K in the vicinity of $z = 0.2$. Values for T_c in the range $0.9 < z < 1.0$ were determined from the DTA measurements [8] and these values are also shown in figure 4. These points clearly do not lie on the same line as the low-z points and, if a second line is drawn through the high z-values, the two lines intersect in the vicinity of $z = 0.6$. This variation in T_N with z is very similar to that shown by the $Cd_xZn_yMn_zTe$ ($x + y + z = 1$) alloys [16]. In that case, the change in slope at about $z = 0.6$ was attributed to a change in behaviour from spin-glass behaviour at low z to antiferromagnetism at higher z and it is possible that similar behaviour occurs in the present alloy system.

Acknowledgments

The authors wish to acknowledge the assistance of Mrs A M Lamarche in the susceptibility and ESR measurements, and Dr D Rancourt and Mr M Royer in the measurement and analysis of the Mössbauer data.

References

[1] Shapira Y, McNiff E J, Oliviera N F, Honig E D, Dwight K and Wold A 1988 *Phys. Rev.* B **37** 7108
[2] Furdyna J K and Kossut J 1988 *Semiconductors and Semimetals* vol 25 (New York: Academic)
[3] Testellin C, Mauger A, Rigaux C, Guillot M and Mycielski A 1989 *Solid State Commun.* **71** 923
[4] Joshi N V and Mogollen L 1985 *Prog. Cryst. Growth Characteristics* **10** 65
[5] Digiuseppe M, Steger J, Wold A and Kostiner E 1974 *Inorg. Chem.* **13** 1828
[6] Teranishi T, Sato K and Saito Y 1977 *Ternary Compounds 1977 (Inst. Phys. Conf. Ser. 35)* ed G P Holah (Bristol: Institute of Physics) p 59
[7] Lamarche G, Woolley J C, Tovar R, Quintero M and Sagredo V 1989 *J. Magn. Magn. Mater.* **80** 321
[8] Brun del Re R, Woolley J C, Quintero M and Tovar R 1990 *Phys. Status Solidi* a **121** 483
[9] Greenwood N N and Whitfield H J 1968 *J. Chem. Soc.* A 1697
[10] Kambara T, Suzuki K and Gondaira K F 1975 *J. Phys. Soc. Japan* **39** 764
[11] Lamarche G 1989 *Rev. Sci. Instrum.* **60** 5
[12] Spalek J, Lewicki A, Tarnawski Z, Furdyna J K, Galazka R R and Obuszko Z 1986 *Phys. Rev.* B **33** 3407
[13] Raj D and Puri S P 1969 *Nuovo Cimento* B **60** 261
[14] Raj D, Chandra K and Puri S P 1968 *J. Phys. Soc. Japan* **24** 39
[15] Wertz J E and Bolton J B 1972 *Electron Spin Resonance* (New York: McGraw-Hill) p 327
[16] Donofrio T, Lamarche G and Woolley J C 1985 *J. Appl. Phys.* **57** 1937
[17] Morrish A H 1966 *The Physical Principles of Magnetism* (New York: Wiley) p 49
[18] Figgis B N 1966 *Introduction to Ligand Fields* (New York: Interscience) p 299
[19] Donnay G, Corliss L M, Donnay J D H, Elliot N and Hastings J M 1958 *Phys. Rev.* **112** 1917
[20] Yoodee K, Woolley J C and Sa-yakanit V 1984 *Phys. Rev.* B **30** 5904
[21] Chehab S and Woolley J C 1987 *Phys. Status Solidi* b **139** 213
[22] Ribbe P H 1982 *Sulfide Mineralogy, Reviews in Mineralogy* No 1 (New York: Bookcrafters) p pr-22
[23] Smart J S 1966 *Effective Field Theories of Magnetism* (Philadelphia, PA: Saunders) p 58
[24] Schneider J, Rauber B and Brandt G 1973 *J. Phys. Chem. Solids* **44** 443